Redox Reactivity of the Binuclear Iron Active Site of Porcine Purple Acid Phosphatase (Uteroferrin)

Manuel A. S. Aquino and A. Geoffrey Sykes*
Department of Chemistry, University of Newcastle, Newcastle upon Tyne, NE1 7RU, UK

Redox interconversions (25 °C) of active $Fe^{II}Fe^{III}$ purple acid phosphatase (PAP_r), and the inactive $Fe^{III}Fe^{III}$ form (PAP_o), have been explored at pH 5.0 (close to maximum activity), I = 0.100 M (NaCl). At this pH the PAP_o–PAP_r couple has a reduction potential $E^{\circ\prime}$ of 367 mV *vs.* normal hydrogen electrode. Whereas with $[Co(phen)_3]^{3+}$ as oxidant for PAP_r first-order dependencies on both reactants are observed (k = 1.26 M^{-1} s^{-1}), with $[Fe(CN)_6]^{3-}$ saturation kinetics are obtained with association, K = 540 M^{-1}, occurring prior to electron transfer, k_{et} = 1.0 s^{-1}. The latter reaction undergoes competitive inhibition with redox inactive $[Cr(CN)_6]^{3-}$ (K_{Cr} = 550 M^{-1}) and $[Mo(CN)_8]^{4-}$ (K_{Mo} = 1580 M^{-1}) consistent with a positively charged locality on the protein surface influencing reactivity. With $[Ru(NH_3)_6]^{2+}$ reduction of PAP_o is too fast to monitor, but with the less strongly reducing $[Ru(NH_3)_5(H_2O)]^{2+}$ a rate law first order in both reactants (k = 2.2 × 10^5 M^{-1} s^{-1}) is observed. Reactions of both these reductants with the less strongly oxidising phosphate bound PAP_o–PO_4 form (183 mV) were also studied. On reduction of PAP_r with $S_2O_4^{2-}$ a bleaching of the colour is observed consistent with $Fe^{II}Fe^{II}$ formation. After 30 min only 40% of the protein could be restored to one or other of the higher oxidation states, indicating loss of Fe^{II}.

The purple acid phosphatases (PAP), alongside haemerythrin, ribonucleotide reductase, and methane monooxygenase are an important category of binuclear iron proteins.[1,2] The phosphatases are known to hydrolyse phosphate esters under acidic conditions.[3] Reactions of nine different phosphates with active $Fe^{II}Fe^{III}$ purple acid phosphatase from porcine uteri (uteroferrin) have already been reported from this laboratory.[4] In addition to $Fe^{II}Fe^{III}$ (PAP_r) there exists an inactive $Fe^{III}Fe^{III}$ form (PAP_o) which can be generated under aerobic conditions, notably in the presence of phosphate. Indeed phosphate bound PAP_o–PO_4 is obtained in about equal amounts along with PAP_r in the isolation procedure. It is of interest therefore to explore factors affecting interconversion of the two redox states. In addition the transfer of Fe from PAP to transferrin has been observed,[5] and alternative roles for the protein have been suggested including Fe transport.

Uteroferrin ($M_r \approx 35\,000$, 318 amino acids) is in the PAP_r form pink, peak λ/nm (ε/M^{-1} cm^{-1}) at 510 (4000), and in the PAP_o form purple 550 (4000).[2,6] The visible band arises from a tyrosine to Fe^{III} ligand-to-metal charge-transfer transition, and this Fe^{III} is more difficult to reduce. Although the spectra are very similar, it is possible to monitor changes between the two states as well as the reactions of $H_2PO_4^-$ with PAP_r to give the phosphate-bound product here indicated as PAP_r–PO_4. Extensive studies of physical properties including NMR,[7,8] EPR,[9,10] Mössbauer,[11,12] resonance Raman,[13,14] extended X-ray absorption fine structure (EXAFS),[15,16] and magnetic susceptibility measurements[14,17-19] have been reported. A crystal structure of the Fe–Zn purple acid phosphatase from kidney bean is in progress.[20] At present however, there is uncertainty about the precise structure of the active sites of the reduced and oxidised forms. The most recent summary in the case of uteroferrin follows an EXAFS study by Que and co-workers.[16] In addition to the iron(III) co-ordinated tyrosine, a histidine is believed to be co-ordinated to each of the irons, and it is likely that the carboxylates of Asp and/or Glu residues are co-ordinated. The existence of a μ-oxo bridge is not certain, and a case has been presented for a carboxylate and hydroxo (or alkoxo) bridge in PAP_r, with a hydroxo and alkoxo (or second hydroxo) bridge in PAP_o–PO_4. The remaining sites in PAP_r are either vacant or contain water (Fig. 1).

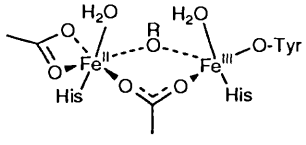

Fig. 1 Possible co-ordination environment in $Fe^{II}Fe^{III}$ purple acid phosphatase

No systematic study of the redox properties of PAP have as yet been reported. Reduction potentials of the PAP_o–PAP_r couple with and without phosphate have been determined at various pH values.[21] The two PAP forms can be interconverted using $[Fe(CN)_6]^{3-}$ or H_2O_2 as oxidant, and ascorbate or β-mercaptoethanol as reductant.[11] In this paper we report kinetic studies on redox interconversions involving PAP_r, PAP_o and PAP_o–PO_4 with various inorganic complexes, and briefly explore the preparation and properties of the fully reduced $Fe^{II}Fe^{II}$ form.

Experimental

Isolation of PAP.—Purple acid phosphatase (uteroferrin) was obtained from the allantoic fluid of sow uteri in mid pregnancy (≈60 d). Purification was carried out using a literature procedure.[6] The UV/VIS absorbance (A) ratio (A_{280}/A_{510}) of the product gave a value < 15 as prescribed. The purified $Fe^{II}Fe^{III}$ (PAP_r) product was dialysed against 40 mM acetate at pH 4.9, and concentrated using an Amicon PM10 filter. Concentrations of protein were determined using molar absorption coefficients (ε) of 4000 M^{-1} cm^{-1} at 510 nm for PAP_r and 550 nm for PAP_o, Fig. 2.

Metal Complexes.—Literature methods were used for the preparation, UV/VIS absorbance spectra peak positions λ/nm (ε/M^{-1} cm^{-1}) for characterisation purposes. The complexes prepared were tris(1,10-phenanthroline)cobalt(III) trichloride heptahydrate, $[Co(phen)_3]Cl_3 \cdot 7H_2O$, 332 (4550);[22] potassium hexacyanochromate(III), $K_3[Cr(CN)_6]$, 308 (58) and 378 (835);[23] potassium octacyanomolybdate(IV), $K_4[Mo(CN)_8]$·

$2H_2O$, 367 (170);[24] and pentaammineaquaruthenium(III) hexafluorophosphate, $[Ru(NH_3)_5(H_2O)][PF_6]_2$.[25] Commercially available potassium hexacyanoferrate(III), $K_3[Fe(CN)_6]$, 420 (1010), was used (BDH, Analar). Hexaammineruthenium(III) chloride, $[Ru(NH_3)_6]Cl_3$, 276 (530) (Johnson Matthey) was further purified by recrystallisation.[26] Hexaammineruthenium(II), 275 (624), was prepared by reducing a solution of hexaammineruthenium(III) chloride on a Jones reductor column under argon.[27] The product was standardised by adding aliquots to an excess of the μ-superoxo-bis[pentaamminecobalt(III)] complex, $[(NH_3)_5Co(O_2)Co(NH_3)_5][ClO_4]_5 \cdot H_2O$, 670 (890 M^{-1} cm^{-1} per dimer),[28] and measuring the change in absorbance for the 1:1 reaction. Relevant reduction potentials for these various reagents are listed in Table 1.

Kinetic Studies.—Reactions were monitored on a Dionex D-110 stopped-flow, or in the case of the $[Co(phen)_3]^{3+}$ reaction a Shimadzu UV2101-PC spectrophotometer. Absorbance changes were followed in the range 600–620 nm, Fig. 2. Solutions of PAP–PO_4 were prepared by treating $H_2PO_4^-$ with PAP_r at pH 5.0 and then air oxidising to PAP_o–PO_4. At this pH the phosphate is believed to be present as a bridging HPO_4^{2-} ligand. Free phosphate is removed by dialysis. Reduction of PAP_o–PO_4 to PAP_r–PO_4 gives a smaller shift in peaks from ≈540 nm to 510 nm. Protein concentrations were in the range (1.5–3.0) × 10^{-5} M and all reactions were carried out at 25.0 ± 0.1 °C and pH 5.0 (40 mM acetate buffer) with ionic strength adjusted to I = 0.100 ± 0.001 M (NaCl). In the case of the ruthenium(II) reactants, solutions were prepared under an inert argon atmosphere. Solutions of PAP_o were dialysed against the buffer purged of O_2–N_2 using argon. Both solutions were loaded onto the stopped-flow under argon. Oxidant or reductant concentrations were in ⩾10 fold excess over the protein. First-order rate constants, k_{obs}, were obtained directly from an OLIS software package interfaced to the stopped-flow, or in the case of the conventional studies from plots of ln $(A_\infty - A_t)$ *vs.* t, which were linear for at least four half-lives.

Results

Oxidation of PAP_r.—*With* $[Co(phen)_3]^{3+}$. The oxidation of PAP_r with $[Co(phen)_3]^{3+}$ studied by conventional spectrophotometry gave first-order rate constants k_{obs}, Table 2. A second-order rate constant of 1.26 ± 0.03 M^{-1} s^{-1} was obtained from the linear plot of k_{obs} against $[Co(phen)_3^{3+}]$ (zero intercept). The range of concentrations could not be extended because at higher concentrations the $[Co(phen)_3]^{3+}$ absorbance obscures that of the protein.

With $[Fe(CN)_6]^{3-}$. First-order rate constant k_{obs}, Table 2, were determined by the stopped-flow spectrophotometry. At the higher $[Fe(CN)_6]^{3-}$ concentrations there was evidence for saturation kinetics, Fig. 3. The protein is basic, pI > 9.6,[13] and in view of the high positive charge at pH 5, association of the oxidant with the protein prior to electron transfer seems a reasonable explanation [equations (1) and (2)].

$$PAP_r + [Fe(CN)_6]^{3-} \overset{K_{Fe}}{\rightleftharpoons} PAP_r\text{–}[Fe(CN)_6]^{3-} \quad (1)$$

$$PAP_r\text{–}[Fe(CN)_6]^{3-} \xrightarrow{k_{et}} PAP_o + [Fe(CN)_6]^{4-} \quad (2)$$

Since $[Fe(CN)_6]^{3-}$ is in >10 fold excess of the protein this gives the dependence (3). A plot of k_{obs}^{-1} against

$$k_{obs} = \frac{k_{et}K_{Fe}[Fe(CN)_6^{3-}]}{1 + K_{Fe}[Fe(CN)_6^{3-}]} \quad (3)$$

$[Fe(CN)_6^{3-}]^{-1}$, inset Fig. 3, is linear, and K_{Fe} and k_{et} can be obtained from the slope and intercept, K = 540 ± 10 M^{-1} and k_{et} = 1.00 ± 0.06 s^{-1}.

Reduction of PAP_o.—*With* $[Ru(NH_3)_6]^{2+}$. The $[Ru(NH_3)_6]^{2+}$ reduction of PAP_o was too fast to monitor by the stopped-flow method. The reduction potential of the protein is less for the phosphate complexed form PAP_o–PO_4, Table 1. This leads to a decrease in the driving force with $[Ru(NH_3)_6]^{2+}$, and the reduction process can now be followed. The final spectrum corresponds to PAP_r (peak at 515 nm) consistent with rapid aquation of the phosphate product. Rate constants k_{obs} are listed in Table 2. A plot of k_{obs} against $[Ru(NH_3)_6^{2+}]$, is linear, Fig. 4. From the slope of Fig. 4, k = (1.80 ± 0.04) × 10^3 M^{-1} s^{-1}.

With $[Ru(NH_3)_5(H_2O)]^{2+}$. In this case the ruthenium(II) reduction has a smaller driving force and the decay of PAP_o could be monitored giving k_{obs}, Table 2. From the slope of a plot of k_{obs} against $[Ru(NH_3)_5(H_2O)^{2+}]$ the second-order rate constant k = (2.2 ± 0.1) × 10^5 M^{-1} s^{-1}. The reduction of PAP_o–PO_4 was also studied, and found to be similar to that with $[Ru(NH_3)_6]^{2+}$. The slope of a plot of k_{obs} against $[Ru(NH_3)_5(H_2O)^{2+}]$, Fig. 4, gives k = 706 ± 8 M^{-1} s^{-1}.

Competitive Inhibition of the $[Fe(CN)_6]^{3-}$ *Oxidation by* $[Cr(CN)_6]^{3-}$ *and* $[Mo(CN)_8]^{4-}$.—The reactions were studied with inhibitor in the oxidant solution prior to mixing. A run

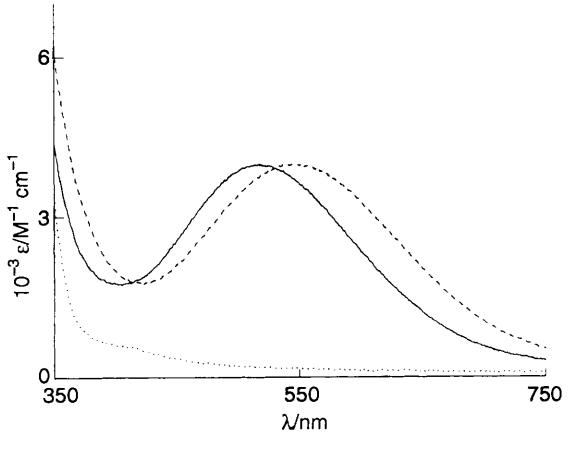

Fig. 2 Visible absorption spectra of purple acid phosphatase uteroferrin in the active $Fe^{II}Fe^{III}$ (——), $Fe^{III}Fe^{III}$ (– – – –) and $Fe^{II}Fe^{II}$ (· · · ·) forms at pH 5.0

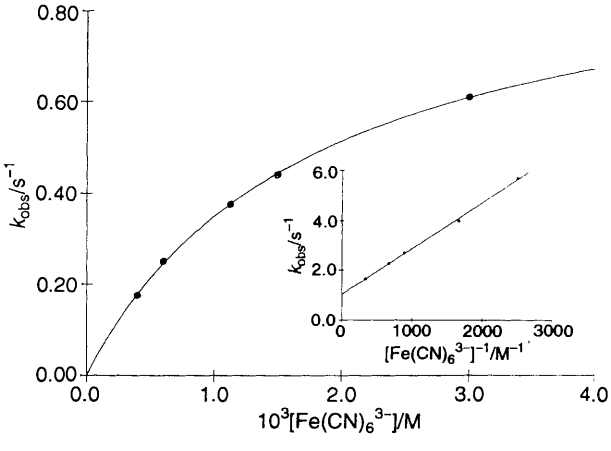

Fig. 3 The variation of first-order rate constants k_{obs} (25 °C) for the $[Fe(CN)_6]^{3-}$ oxidation of purple acid phosphatase (uteroferrin) $Fe^{II}Fe^{III}$, PAP_r, with $[Fe(CN)_6^{3-}]$, and (inset) the reciprocal plot indicating the nature of the dependence at pH 5.0, I = 0.100 M (NaCl)

Table 1 Listing of reduction potentials *vs.* NHE (normal hydrogen electrode) at 25 °C, I = 0.10 M except where indicated

Couple	$E°'$/mV	Comments
PAP_o–PAP_r (Uf)	367	pH 5.0 (acetate); I = 0.26 M, ref. 21
PAP_o–PO_4/PAP_r–PO_4 (Uf)	183	pH 5.0 (acetate); I = 0.26 M, ref. 21
$[Co(phen)_3]^{3+/2+}$	370	Ref. 29
$[Fe(CN)_6]^{3-/4-}$	410	Ref. 30
$[Ru(NH_3)_5(H_2O)]^{3+/2+}$	67	Ref. 31; I = 0.20 M
$[Ru(NH_3)_6]^{3+/2+}$	50	

Table 2 First-order rate constants k_{obs} (25 °C) for redox interconversion of $Fe^{II}Fe^{III}$ (PAP_r) and $Fe^{III}Fe^{III}$ (PAP_o) forms of porcine purple acid phosphatase (uteroferrin), concentrations (1.2–2.8) × 10^{-5} M, at pH 5.0, I = 0.100 M (NaCl)

PAP_r + $[Co(phen)_3]^{3+}$					
$10^4[Co(phen)_3^{3+}]$/M	2.9	4.1	6.0		
k_{obs}/s^{-1}	3.5	5.0	7.6		
PAP_r + $[Fe(CN)_6]^{3-}$					
$10^4[Fe(CN)_6^{3-}]$/M	4.0	6.0	11.3	15.0	30.0
k_{obs}/s^{-1}	0.175	0.250	0.375	0.440	0.610
$[Ru(NH_3)_6]^{2+}$					
$10^4[Ru(NH_3)_6^{2+}]$/M	1.62	3.45	5.96	7.44	10.3
k_{obs}/s^{-1}	0.275	0.560	1.09	1.33	1.81
$[Ru(NH_3)_5(H_2O)]^{2+}$ + PAP_o–PO_4					
$10^4[Ru(NH_3)_5(H_2O)^{2+}]$/M	2.03		5.06	8.09	10.1
k_{obs}/s^{-1}	0.134		0.34	0.56	0.71
$[Ru(NH_3)_5(H_2O)]^{2+}$ + PAP_o					
$10^4[Ru(NH_3)_5(H_2O)^{2+}]$/M	2.03	3.50	5.06		
k_{obs}/s^{-1}	38	73	110		

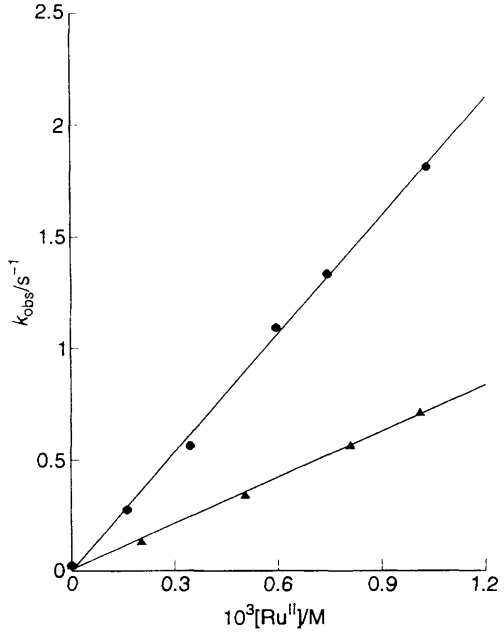

Fig. 4 The linear dependence of first-order rate constants k_{obs} (25 °C) for the $[Ru(NH_3)_6]^{2+}$ (●) and $[Ru(NH_3)_5(H_2O)]^{2+}$ (▲) reductions of the purple acid phosphatase (uteroferrin) phosphate-bound $Fe^{III}Fe^{III}$ forms, PAP_o–PO_4, at pH 5.0, I = 0.100 M (NaCl)

performed with $[Cr(CN)_6]^{3-}$ in the protein solution gave identical behaviour. Rate constants k_{obs} for the oxidation of PAP_r decrease in the presence of redox inactive $[Cr(CN)_6]^{3-}$, (0.5–5.0) × 10^{-3} M, and $[Mo(CN)_8]^{4-}$, (0.5–3.0) × 10^{-3} M, Table 3 as illustrated in Fig. 5. The effect can be accounted for by equations (4) and (5) where B is the inhibitor or blocking agent. Concentrations of $[Fe(CN)_6]^{3-}$ were at the lower end of the range explored, so that association of $[Fe(CN)_6]^{3-}$ with PAP_r was minimised. Hence, reaction independent of B could be represented by the second-order process k_1, (5). This reaction sequence gives the expression (6).

$$PAP_r + B \underset{}{\overset{K_{Cr}}{\rightleftharpoons}} PAP_r\text{–}B \quad (4)$$

$$PAP_r + [Fe(CN)_6]^{3-} \xrightarrow{k_1} \text{products} \quad (5)$$

$$k_{obs} = \frac{k_1[Fe(CN)_6^{3-}]}{1 + K_{Cr}[Cr(CN)_6^{3-}]} \quad (6)$$

A plot of $[Fe(CN)_6^{3-}]/k_{obs}$ against $[Cr(CN)_6^{3-}]$, Fig. 5, gives k_1 = 490 ± 10 M^{-1} s^{-1}, and K_{Cr} = 550 ± 25 M^{-1}. The corresponding plot for $[Mo(CN)_8]^{4-}$ gives k_1 = 500 ± 15 M^{-1} and K_{Mo} = 1580 ± 110 M^{-1}.

Reduction of PAP_r *with* $S_2O_4^{2-}$.—The reduction of PAP_r can be achieved by addition of dithionite, final pH 5.0. With dithionite at 0.5 mM decay of the 510 nm band requires ≈30 min at 25 °C. Subsequent addition of H_2O_2 gave only 40% recovery, with the product peak at 560 nm corresponding to formation of PAP_o.

Discussion

The catalytic activity of purple acid phosphatase is very much dependent on the oxidation state of the binuclear iron centre, with the mixed-valent $Fe^{II}Fe^{III}$ form providing activity towards the hydrolysis of phosphate esters, and the $Fe^{III}Fe^{III}$ form inactive. Indeed, the facile interconversion between redox states may be used to control phosphatase activity.[32] Aerobic conversion of PAP_r to PAP_o in the absence of phosphate requires >1 week, and in the presence of phosphate is somewhat faster with a rate constant (25 °C) of 6.8 × 10^{-5} s^{-1} at pH 5.0.[4]

In the present study we have shown that the interconversion of PAP_r and PAP_o with and without phosphate attached can be readily brought about by inorganic complexes, Table 4. The reduction potential for the PAP_o–PAP_r couple at pH 5.0 is 367 mV,[21] and the driving force favours oxidation of PAP_r with $[Fe(CN)_6]^{3-}$ (410 mV) and $[Co(phen)_3]^{3+}$ (370 mV). In the

Table 3 The effects of redox inactive $[Cr(CN)_6]^{3-}$ and $[Mo(CN)_8]^{4-}$ on rate constants k_{obs} (25 °C) for the $[Fe(CN)_6]^{3-}$ oxidation of porcine $Fe^{II}Fe^{III}$, PAP_r in the range (1.0–1.4) × 10^{-5} M at pH 5.0, I = 0.100 M (NaCl)

$10^3[Cr(CN)_6^{3-}]$/M	0	0.5	1.0	2.0	3.0	4.0	5.0
$10^2k_{obs}/s^{-1}$	7.7	5.7	4.8	3.6	2.9	2.5	2.1
$10^3[Mo(CN)_8^{4-}]$/M	0	0.5	1.0	1.5	2.0	2.5	3.0
$10^2k_{obs}/s^{-1}$	5.7	2.90	2.11	1.80	1.47	1.22	1.05

Table 4 Summary of kinetic data for redox interconversions of $Fe^{II}Fe^{III}$ (PAP_r) and $Fe^{III}Fe^{III}$ (PAP_o) forms of purple acid phosphatase (uteroferrin) at pH 5.0, I = 0.100 M (NaCl)

Reaction	$k/M^{-1}\ s^{-1}$	k_{et}/s^{-1}	K/M^{-1}
$PAP_r + [Co(phen)_3]^{3+}$	1.26		
$PAP_r + [Fe(CN)_6]^{3-}$		1.0	540
$PAP_r + [Cr(CN)_6]^{3-}$			550
$PAP_r + [Mo(CN)_8]^{4-}$			1580
$[Ru(NH_3)_6]^{2+} + PAP_o$–$PO_4$	1.8×10^3		
$[Ru(NH_3)_5(H_2O)]^{2+} + PAP_o$–$PO_4$	706		
$[Ru(NH_3)_5(H_2O)]^{2+} + PAP_o$	2.2×10^5		

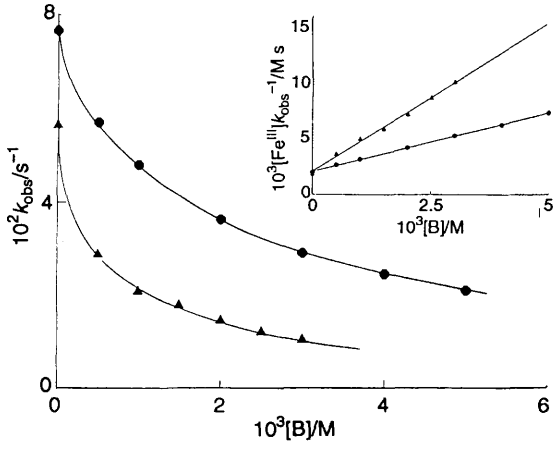

Fig. 5 The competitive inhibition of the $[Fe(CN)_6]^{3-}$ oxidation of purple acid phosphatase (uteroferrin) $Fe^{II}Fe^{III}$, PAP_r by redox inactive inhibitors [B] = $[Cr(CN)_6]^{3-}$ (●) and $[Mo(CN)_8]^{4-}$ (▲), and (inset) the plot indicating the nature of the dependence at pH 5.0, I = 0.100 M (NaCl)

case of $[Fe(CN)_6]^{3-}$ saturation kinetics are observed which can be interpreted in terms of association K_{Fe} = 540 M^{-1} prior to electron transfer k_{et} = 1.0 s^{-1}. The same mechanism may well apply in the case of $[Co(phen)_3]^{3+}$, in which case k ($=k_{et}K$) is 1.26 $M^{-1}\ s^{-1}$, but since saturation kinetics are not observed there is no means of separating the smaller K and k_{et}.

Uteroferrin is a highly basic protein (pI > 9.6), and from the amino-acid composition at pH 5.0 the charge can be estimated as +33, assuming 1+ for Arg, Lys, His and 1− for Asp and Glu residues. The association constant K_{Fe} for PAP_r with $[Fe(CN)_6]^{3-}$ of 540 M^{-1} indicates the influence of a region of positive charge on the protein surface in close proximity to the active site. From the $[Cr(CN)_6]^{3-}$ inhibition of the $[Fe(CN)_6]^{3-}$ reaction an association constant K_{Cr} = 550 M^{-1} is obtained, in good agreement with K_{Fe}, and in the case of $[Mo(CN)_8]^{4-}$ the higher K_{Mo} = 1580 M^{-1} is clearly supportive of an electrostatic effect. Thus a self-consistent interpretation is possible and may be extended to include a consideration of phosphate ester reactants with an overall negative charge, which presumably take advantage of the positive charge in a similar manner. There is as yet no information from X-ray crystallography concerning the structure of the protein, and whether the active site is at the surface or located in a pocket. Penetration of the protein and accessing of the active site by $Fe(CN)_6]^{3-}$ is not envisaged, since the interaction of $[Fe(CN)_6]^{3-}$ with Fe^{II} would be expected to give a shift in colour. Rather an interaction of $[Fe(CN)_6]^{3-}$ at a positively charged region on the protein surface at or close to the point of entry to the pocket containing the active site is envisaged. The magnitude of the association constants K_{Fe}, K_{Cr} and K_{Mo} suggests a localised protein charge of ≈4+.[33]

Reduction of both PAP_o and PAP_o–PO_4 by $[Ru(NH_3)_5(H_2O)]^{2+}$ and $[Ru(NH_3)_6]^{2+}$ gives PAP_r as the final product (λ_{max} = 515 nm). In the case of PAP_o–PO_4 reduction is followed by rapid dissociation of the bound phosphate, since the amount of free phosphate is small, and PAP_r–PO_4 is quite labile.[4] Again there is no evidence for an inner-sphere reaction with $[Ru(NH_3)_5(H_2O)]^{2+}$ at either the Fe^{III}_2 active site or *e.g.* a surface histidine, which would result in retention of the ruthenium(III) product. The larger rate constant of 1800 $M^{-1}\ s^{-1}$ observed for $[Ru(NH_3)_6]^{2+}$ (which has the higher driving force) as compared to $[Ru(NH_3)_5(H_2O)]^{2+}$ (706 $M^{-1}\ s^{-1}$) is consistent with identical mechanisms.[34] Since the $[Ru(NH_3)_6]^{2+}$ reaction must be outer-sphere this suggests that the $[Ru(NH_3)_5(H_2O)]^{2+}$ reaction adopts a similar mechanism. The redox activity observed in this study compares with the inactivity of haemocyanin (M_r = 78 000) with inorganic complexes. Assuming that reorganisation at the binuclear metal ion centres is about the same and a distance dependence for electron-transfer rate constants applies,[35] this suggests that the active site of PAP is not as buried as is the case in haemocyanin.[36] Although the positively charged region on PAP favours anionic reactants, it is notable that cationic reactants retain an appreciable reactivity.

Finally we have attempted to apply the Marcus equation (7)[37] to the reactions here studied, where k_{11} and k_{22} are

$$k_{12} = (k_{11}k_{22}K_{12}f)^{\frac{1}{2}}W_{12} \quad (7)$$

self-exchange rate constants for the respective couples, k_{12} the rate constant for the cross-reaction (equilibrium constant K_{12}), and the constant f and work-term coefficient W_{12} are both assumed to be unity. With redox partners $[Co(phen)_3]^{3+}$ and $[Fe(CN)_6]^{3-}$ the PAP_r + PAP_o self-exchange rate constant can be calculated as 5.6 $M^{-1}\ s^{-1}$ and 0.035 $M^{-1}\ s^{-1}$ respectively. In the case of $[Ru(NH_3)_5(H_2O)]^{2+}$ no self-exchange rate constant is available. Without allowances for W_{12} the simple Marcus theory does not appear to hold very well.

Acknowledgements

We thank NATO/Natural Sciences and Engineering Research Council of Canada for post-doctoral support (M. A. S. A.).

References

1 J. B. Vincent, G. L. Olivier-Lilley and B. A. Averill, *Chem. Rev.*, 1990, **90**, 1447.
2 R. G. Wilkins, *Chem. Soc. Rev.*, 1992, **21**, 171.
3 B. C. Antanaitis and P. Aisen, *Adv. Inorg. Biochem.*, 1983, **5**, 111.
4 M. A. S. Aquino, J.-S. Lim and A. G. Sykes, *J. Chem. Soc., Dalton Trans.*, 1992, 2135; 1994, 429.
5 P. R. Nuttleman and R. M. Roberts, *J. Biol. Chem.*, 1990, **265**, 12192.
6 J. W. Pyrz, J. T. Sage, P. G. Debrunner and L. Que, jun., *J. Biol. Chem.*, 1986, **261**, 11015.
7 R. C. Scarrow, J. W. Pyrz and L. Que, jun., *J. Am. Chem. Soc.*, 1990, **112**, 657.

8 Z. Wang, L.-J. Ming, L. Que, jun., J. B. Vincent, M. W. Crowder and B. A. Averill, *Biochemistry*, 1992, **31**, 5263.
9 B. C. Antanaitis, J. Peisach, W. B. Mims and P. Aisen, *J. Biol. Chem.*, 1985, **260**, 4572.
10 M. W. Crowder, J. B. Vincent and B. A. Averill, *Biochemistry*, 1992, **31**, 9603.
11 P. G. Debrunner, M. P. Hendrich, J. De Jersey, D. T. Keough, J. T. Sage and B. Zerner, *Biochim. Biophys. Acta*, 1983, **745**, 103.
12 K. Chichutek, H. Witzel and F. Parak, *Hyperfine Interact.*, 1988, **42**, 885.
13 B. P. Gaber, J. P. Sheridon, F. W. Bazer and R. M. Roberts, *J. Biol. Chem.*, 1979, **254**, 8340.
14 B. A. Averill, J. C. Davis, S. Burmann, T. Zinno, J. Sanders-Loehr, T. M. Loehr, J. T. Sage and P. G. Debrunner, *J. Am. Chem. Soc.*, 1987, **109**, 3760.
15 S. M. Kauzlarich, B. K. Teo, S. Burmann, J. C. Davis and B. A. Averill, *Inorg. Chem.*, 1986, **25**, 2781.
16 A. E. True, R. C. Scarrow, C. R. Randall, R. C. Holz and L. Que, jun., 1993, **115**, 4246.
17 J. C. Davis and B. A. Averill, *Proc. Natl. Acad. Sci. USA*, 1982, **79**, 4623.
18 J. L. Beck, L. A. McConachie, A. C. Summers, W. N. Arnold, J. De Jersey and B. Zerner, *Biochim. Biophys. Acta*, 1986, **869**, 61.
19 E. P. Day, S. S. David, J. Peterson, W. R. Dunham, J. J. Bonvoisin, R. M. Sands and L. Que, jun., *J. Biol. Chem.*, 1988, **263**, 15561.
20 N. Sträter, R. Fröhlich, A. Schiemann, B. Krebs, M. Körner, H. Suerbaum and H. Witzel, *J. Mol. Biol.*, 1992, **224**, 511.
21 D. L. Wang, R. C. Holz, S. S. David, L. Que, jun., and M. T. Stankovich, *Biochemistry*, 1991, **30**, 8187.
22 D. Pfeiffer and B. Werdelmann, *Z. Anorg. Allg. Chem.*, 1950, **263**, 31.
23 J. H. Bigelow, *Inorg. Synth.*, 1946, **2**, 203.
24 J. Van der Poil and H. M. Newmann, *Inorg. Synth.*, 1968, **11**, 53.
25 J. C. Curtis, B. P. Sullivan and T. J. Meyer, *Inorg. Chem.*, 1983, **22**, 224.
26 G. Navon and N. Sutin, *Inorg. Chem.*, 1974, **13**, 2159.
27 D. E. Harrison and H. Taube, *J. Am. Chem. Soc.*, 1967, **89**, 5706.
28 R. Davies, M. Mori, A. G. Sykes and J. A. Weil, *Inorg. Synth.*, 1970, **12**, 197.
29 S. K. Chapman, C. V. Knox, P. Kathirgamanathan and A. G. Sykes, *J. Chem. Soc., Dalton Trans.*, 1984, 2769.
30 J. Butler, M. D. Davies and A. G. Sykes, *J. Inorg. Biochem.*, 1981, **15**, 41.
31 T. Matsubara and P. C. Ford, *Inorg. Chem.*, 1976, **15**, 1107.
32 J. B. Vincent and B. A. Averill, *Faseb J.*, 1990, **4**, 3009.
33 S. K. Chapman, J. D. Sinclair-Day, A. G. Sykes, S.-C. Tam and R. J. P. Williams, *J. Chem. Soc., Chem. Commun.*, 1983, 1152.
34 B.-J. Zhang, C. R. Andrew, N. P. Tomkinson and A. G. Sykes, *Biochim. Biophys. Acta*, 1992, **1102**, 245.
35 C. C. Moser, J. M. Keske, K. Warncke, R. S. Farid and P. L. Dutton, *Nature (London)*, 1992, **235**, 796.
36 K. A. Magnus and T.-T. Hoa, *J. Inorg. Biochem.*, 1992, **47**, 20; A. Volbeda and W. G. J. Hol, *J. Mol. Biol.*, 1989, **209**, 249.
37 R. A. Marcus and N. Sutin, *Biochem. Biophys. Acta*, 1985, **811**, 265.

Received 19*th July* 1993; *Paper* 3/04225A